Reversal of Nonlocal Vortex Motion in the Regime of Strong Nonequilibrium

Florian Otto,[1,*] Ante Bilušić,[1,2] Dinko Babić,[3] Denis Yu. Vodolazov,[4] Christoph Sürgers,[5] and Christoph Strunk[1]

[1]*Institute for Experimental and Applied Physics, University of Regensburg, D-93025 Regensburg, Germany*
[2]*Faculty of Natural Sciences, University of Split, N. Tesle 12, HR-21000 Split, Croatia*
[3]*Department of Physics, Faculty of Science, University of Zagreb, Bijenička 32, HR-10000 Zagreb, Croatia*
[4]*Institute for Physics of Microstructures, Russian Academy of Sciences, 603950, Nizhny Novgorod, GSP-105, Russia*
[5]*Karlsruhe Institute of Technology, Physikalisches Institut and Center for Functional Nanostructures, D-76128 Karlsruhe, Germany*
(Received 17 June 2009; published 14 January 2010)

We investigate nonlocal vortex motion in weakly pinning a-NbGe nanostructures, which is driven by a transport current I and remotely detected as a nonlocal voltage V_{nl}. At a high I of a given polarity, V_{nl} changes sign dramatically. This is followed by V_{nl} becoming even in I, with the opposite sign at low and high temperatures T. These findings can be explained by a Nernst-like effect resulting from local electron overheating (low T), and a magnetization enhancement due to a nonequilibrium quasiparticle distribution that leads to a gap enhancement near the vortex core (high T).

PACS numbers: 74.25.Uv, 74.25.F−, 74.78.Na

When vortices in type II superconductors are strongly driven by a transport current, the quasiparticle distribution function assumes a nonequilibrium form [1–3]. Close to the critical temperature T_c, quasiparticles within rapidly moving vortex cores gain energy by heating and can escape out, while those outside the cores remain unaffected. This behavior—the Larkin-Ovchinnikov (LO) effect—leads to a *shrinkage* of the cores and to a decrease of the vortex-motion viscosity coefficient η [1]. At low T, the entire quasiparticle subsystem is heated by the vortex motion because of the larger electron-phonon collision time. This results in an *expansion* of the cores instead of their shrinkage, while η again decreases [2,3]. In both cases, the current-voltage [$V(I)$] characteristics are very nonlinear and, in fact, so similar that the difference can be resolved only via a quantitative analysis [4,5]. However, vortex shrinkage and vortex expansion are different processes and should lead to qualitative differences in other properties.

In this Letter, we exploit recently discovered nonlocal vortex flow in the *transversal* flux transformer (TFT) geometry [6,7] as a diagnostic tool, which permits an unambiguous distinction of the above two opposite types of nonequilibrium at high and low T. Our sample, shown in the inset to Fig. 1(a), consists of a vertical channel, of length L and width W, and the contacts 1–4. We apply I between 1 and 2 (local lead) and measure V_{nl}, which is a consequence of vortex motion along the channel, between 3 and 4. According to our analysis, vortices are at high I set in motion either by a gradient of T (at low T) or by a gradient of magnetization M (close to T_c) at the interface of the local lead and the channel. The effect close to T_c can be explained by an enhanced dia-magnetism in the LO state, which has eluded observation so far. The low T behavior belongs to the class of Nernst-like effects, and results from electron overheating in the local lead.

Previously, $V_{nl}(I)$ was investigated in the linear response regime [6,7], the main features being accountable for by a model elaborated in Ref. [7] and outlined below. There are $n_\phi WL$ vortices in the channel, where $n_\phi = B/\phi_0$ is the
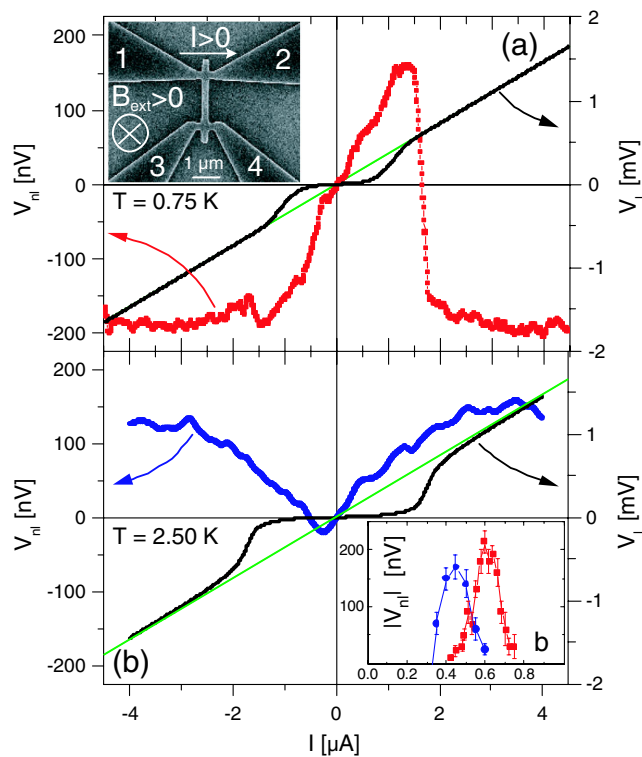

FIG. 1 (color online).   Typical local (black lines; the green [light gray] lines represent the normal-state voltage) and nonlocal (red [medium gray] and blue [dark gray] symbols) $V(I)$ curves. (a) $T = 0.75$ K $= 0.26 T_c$ (at $B_{ext} = 3.0$ T, $b = 0.64$), and (b) $T = 2.50$ K $= 0.85 T_c$ (at $B_{ext} = 0.50$ T, $b = 0.50$). Inset to (a): Sample geometry; $L = 2$ μm, $W = 250$ nm. Inset to (b): Saturation voltages of $|V_{nl}|$, plotted against b, for low (red [medium gray]) and high (blue [dark gray]) T.

vortex density, ϕ_0 the magnetic flux quantum, $B = B_{ext} + \mu_0 M$, B_{ext} the external magnetic field, and $\mu_0 = 4\pi \times 10^{-7}$ V s/A m. The transport current density **j** decreases exponentially away from the local lead, with a decay length $W/\pi \ll L$ [6,8], so most of the vortices in the channel are out of its reach. They can move only in response to the magnetic pressure p exerted by vortices in the area adjacent to the channel, which are driven by a force f_{dr} (per unit vortex length d). If f_{dr} acts towards the channel over a distance X, around $n_\phi WX$ vortices contribute to p, hence $p = (n_\phi WX)(f_{dr}/W)$. The resulting force pWd is balanced by the total frictional force $(n_\phi WL) \times (\eta u_{nl} d)$ on the vortices in the channel (which move at velocity u_{nl}). For a superconductor with a large Ginzburg-Landau (GL) parameter κ, we can approximate $n_\phi \approx B_{ext}/\phi_0$ and use $V_{nl} = WB_{ext}u_{nl}$ to obtain

$$V_{nl} = WB_{ext}Xf_{dr}/\eta L. \tag{1}$$

At low I, i.e., close to equilibrium, f_{dr} is the Lorentz force $f_L = j\phi_0$, assuming $j = |\mathbf{j}| = I/Wd$. In Ref. [7], $X = W$ led to $V_{nl} = (WB_{ext}\phi_0/\eta Ld)I = R_{nl}I$. This reproduced the observed $V_{nl} \propto I$ and $V_{nl} \propto 1/L$ even in the presence of pinning [9].

Our $d = 40$ nm thick a-Nb$_{0.7}$Ge$_{0.3}$ sample [inset to Fig. 1(a); $L = 2$ μm, $W = 250$ nm] was produced by electron-beam lithography and magnetron sputtering onto an oxidized Si substrate [4,8]. The local dissipation was probed by passing I between 1 and 3, and measuring a voltage V_l between 2 and 4. Since W is also the width of the local lead close to the channel, $V_l(I)$ and $V_{nl}(I)$ can be compared directly because the effective j can be considered to be essentially the same in both cases. Measurements of $V_l(I)$ provided all relevant parameters of our samples: $T_c = 2.94$ K, the normal-state resistivity $\rho_n = 1.82$ $\mu\Omega$m, $-(dB_{c2}/dT)_{T=T_c} = 2.3$ T/K, where B_{c2} is the equilibrium upper critical magnetic field, and the GL parameters $\kappa = 72$, $\xi(0) = 7.0$ nm, and $\lambda(0) = 825$ nm. The low pinning in a-Nb$_{0.7}$Ge$_{0.3}$ allowed for dc measurements of $V_{nl} \sim 10$–200 nV, which was at the level of $R_{nl} \sim 0.1$ Ω in the low-I linear regime. All measurements were carried out in a ^{3}He cryostat, with B_{ext} perpendicular to the film plane.

Typical results for the two limiting cases of low ($T = 0.75$ K $= 0.26T_c$) and high ($T = 2.50$ K $= 0.85T_c$) temperatures are shown in Figs. 1(a) and 1(b), respectively. The $V_l(I)$ curves exhibit a nonlinear shape characteristic of strong nonequilibrium (SNEQ), originating either in (a) electron heating [2,4,5] or (b) LO vortex-core shrinking [1,4,5]. On the other hand, $V_{nl}(I)$ displays the previously observed linear, antisymmetric dependence [i.e., $V_{nl}(-I) = -V_{nl}(I)$] only at low I. Upon increasing I, sudden sign reversals of V_{nl} are observed in both regimes: at a certain I, the antisymmetric signal converts into a symmetric one. The sign of V_{nl} can be unambiguously attributed to the following directions in the inset to Fig. 1(a): at low positive (negative) I, the positive (negative) V_{nl} corre-

sponds to vortex motion upwards (downwards) in the channel. When I is high, vortices move either downwards ($T \ll T_c$, $V_{nl} < 0$), or upwards ($T \to T_c$, $V_{nl} > 0$), irrespective of the direction of I. The saturation values of $|V_{nl}|$ at high I are plotted vs $b = B_{ext}/B_{c2}$ in the inset to Fig. 1(b). In both cases, nonzero values are observed only at intermediate b, with a maximum efficiency around $b = 0.6$ ($b = 0.45$) at low (high) T, similarly to the previously observed B_{ext} sweep traces of V_{nl} at low I [6,7]. As argued in Ref. [7], the vanishing of V_{nl} at low B_{ext} is presumably related to increasing the pinning efficiency as B_{ext} (and/or T) decreases, whereas $V_{nl}(B_{ext} \to B_{c2}) \to 0$ because the sample goes to the normal state.

We first discuss the regime $T \ll T_c$. Assigning the corresponding high-j SNEQ state to electron heating to $T = T^*$ above the bath temperature T_0 was successful in explaining the measured $V_l(I)$ of Refs. [2,4,5]. An analysis of the present $V_l(I)$ [8] within the same framework permits us to extract $T^*(V_l)$ and, using $V_l(I)$, also $T^*(I)$, which is more convenient for a comparison with the $V_{nl}(I)$ data (see below). The hot electrons penetrate into the channel, which remains at $T = T_0$, roughly up to $L_T = \sqrt{D\tau_0} \approx 295$ nm $\sim W$. Here, $D = 4.80 \times 10^{-5}$ m^2/s is the diffusion constant, and $\tau_0 \approx 1.82$ ns is the relaxation time of the hot electrons, resulting from the mentioned analysis [8]. Hence, there is a T gradient which leads to a thermal driving force $\mathbf{f}_T = -S_\phi \nabla T$ and consequently to the Nernst effect. S_ϕ is the vortex transport entropy [10]. The Nernst effect should lead to vortex motion downwards, which agrees with the observed $V_{nl} < 0$. Since $T^* - T_0 \sim 1$ K typically, the observed temperature gradients $|\nabla T| \sim (T^* - T_0)/L_T \sim 1$ K/μm are much larger than in usual measurements of the Nernst effect.

The above is elaborated in Fig. 2, where the result for $B_{ext} = 3.0$ T ($b = 0.64$) is analyzed more closely. The shape of $V_{nl}(I)$ in Fig. 1(a) suggests that we consider the symmetric ($+$) and antisymmetric ($-$) parts of V_{nl} separately via $V_{nl}^\pm(I) = [V_{nl}(I) \pm V_{nl}(-I)]/2$, which is shown in Fig. 2(a). $V_{nl}^-(I)$ at low I is fairly linear as expected, since $f_{dr} = f_L$, while $V_{nl}^+(I)$ is very small. When I is increased further, $V_{nl}^-(I)$ rapidly decreases and $V_{nl}^+(I) < 0$ simultaneously grows to a constant value comparable to that of the maximum $V_{nl}^-(I) > 0$. This dramatic change occurs around I where V_l assumes the normal-state value [see Fig. 1(a)], signifying the transition to the normal state in the local region [4,5] and consequent vanishing of f_L. Furthermore, $|I|$ where V_{nl} steeply changes sign on the $I > 0$ side ($\mathbf{f}_L$ and $\mathbf{f}_T$ act oppositely) coincides with $|I|$ where V_{nl} has a local minimum on the $I < 0$ side ($\mathbf{f}_L$ and $\mathbf{f}_T$ add); this is consistent with only $\mathbf{f}_T$ remaining effective at higher $|I|$.

In the main panel of Fig. 2(b), we plot $T^*(I)$ extracted according to the electron heating model [4,5] in the superconducting state and from noise measurements in the normal state [8], whereas in the inset we show a sketch of the T profile along the sample. One can see that the
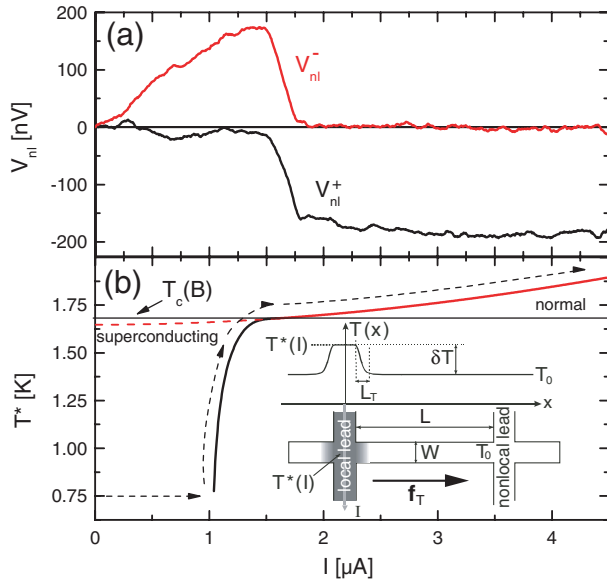
FIG. 2 (color online). (a) Measured V_{nl} at $T \ll T_c$: antisymmetric (red) and symmetric (black) part of the nonlocal signal at $T = 0.75$ K and $B_{ext} = 3.0$ T. (b) Effective electron temperature $T^*(I)$, where the black line stems from an analysis of $V_l(I)$, and the red line from noise measurements in the normal state [8]. Inset: Sketch of the temperature profile along the channel.

electron heating is basically absent at low I, then sets in very steeply until it reaches $T_c(B_{ext})$ that represents $B_{c2}(T)$ [4,5,8], after which it changes with I only weakly. The nearly flat $V_{nl}^+(I)$ at high I hence corresponds to $T^* \approx T_c(B_{ext})$, so $|\nabla T| \approx [T_c(B_{ext}) - T_0]/L_T = \delta T/L_T$. Using Eq. (1), we can extract S_ϕ from our data by focusing on the saturating values of $V_{nl}^+(I)$. We approximate $f_{dr} = f_T \approx S_\phi \delta T/L_T$ and $X \approx L_T$ to obtain

$$S_\phi = V_{nl}\phi_0/R_{nl}\delta Td, \qquad (2)$$

which does not contain L_T. In the (B_{ext}, T) range of our data, we find $S_\phi \sim 0.03$–0.5×10^{-12} J m^{-1} K^{-1}, which is in reasonable agreement with a theoretical estimate ~ 0.1–0.2×10^{-12} J m^{-1} K^{-1} from the Maki formula [11,12], as well as with experimental data on films of Nb $(0.05$–1.5×10^{-12} J m^{-1} K$^{-1})$ [13] and of Pb-In $(0.2$–5×10^{-12} J m^{-1} K$^{-1})$ [14].

We now turn to the regime $T \to T_c$. An analysis [8] of the $V_l(I)$ in the spirit of Refs. [4,5] reveals that this SNEQ state corresponds to the LO vortex-core shrinking [1], with $T \approx T_0$ everywhere because electron heating is strongly suppressed close to T_c [2,4,5]. $V_l(I)$ for $T \ll T_c$ and $T \to T_c$ are at first glance rather similar, so the difference becomes obvious only through a numerical analysis [4,5]. In contrast, the qualitatively different $V_{nl}(I)$ curves in Fig. 1 leave no doubt that we are dealing with two distinct SNEQ phenomena. As before, the shape of $V_{nl}(I)$ [see Fig. 1(b)] suggests that we consider $V_{nl}^+(I)$ and $V_{nl}^-(I)$ separately, which is shown in Figs. 3(a) and 3(b), respectively. $V_{nl}^-(I)$ at low I is linear for small b, which implies the
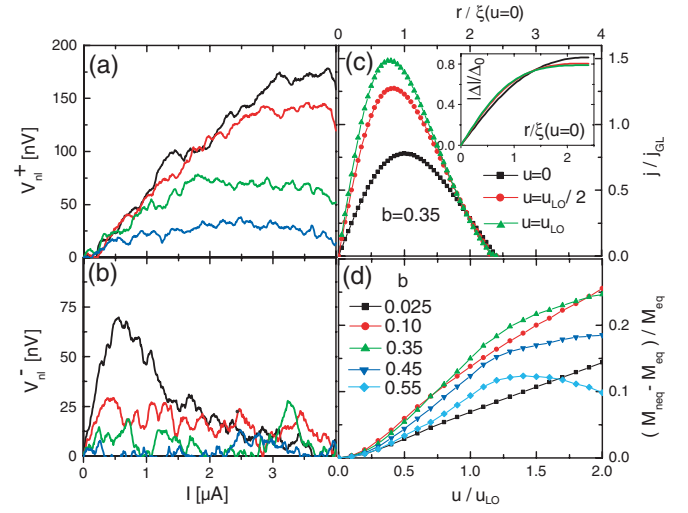

FIG. 3 (color). Measured $V_{nl}^+(I)$ (a), and $V_{nl}^-(I)$ (b) at $T = 2.50$ K $= 0.85T_c$ and $b = 0.45$ (black), 0.50 (red), 0.55 (green) and 0.60 (blue). (c) Calculated j_s/j_{GL} and $|\Delta|/\Delta_0$ (inset) vs $r/\xi(u = 0)$ for different u/u_{LO}. (d) Calculated $(M_{neq} - M_{eq})/M_{eq}$ against u/u_{LO} at different b (as indicated).

presence of f_L, whereas this is difficult to claim for higher b where the signal is small over the entire I range. At high I, however, $V_{nl}^-(I)$ is small regardless of b. $V_{nl}^+(I)$, on the other hand, increases with increasing I, and eventually saturates at a value comparable to that of the maximum Nernst signal at low T, albeit with the opposite sign. The smallness of $V_{nl}^-(I)$ at high I reflects that of f_L in this regime. This can be understood from the fact that the V_l for these I is not much below the normal state value [see Fig. 1(b)], which means that most of the current is normal [1] and does not contribute to f_L.

Since f_L is negligible and $T \approx T_0$, there must be yet another driving force which governs the TFT effect at high I. Below we show that this force has the same origin as the LO effect on $V_l(I)$, that is, a deviation $\delta g(\epsilon)$ of the quasiparticle distribution function $g(\epsilon)$ from $g_{eq}(\epsilon) = \tanh(\epsilon/2k_BT) = g(\epsilon) - \delta g(\epsilon)$ in equilibrium. An additional consequence of δg is an enhancement of the supercurrent density j_s flowing around the vortex core, which can be calculated following [1,15]

$$\mathbf{j}_s = \frac{1}{\rho_n e}\left(\frac{\pi}{4k_BT_c}|\Delta|^2 + \frac{\pi}{2}|\Delta|\delta g(|\Delta|)\right)\left(\nabla\varphi - \frac{2e}{\hbar}\mathbf{A}\right), \qquad (3)$$

where $\Delta = |\Delta|\exp(i\varphi)$ is the order parameter and $\mathbf{A}$ the vector potential. The term $\propto |\Delta|^2$ corresponds to the equilibrium contribution to $\mathbf{j}_s$ in the GL model, and the term $\propto \delta g$ to the SNEQ correction. δg is positive for energies less than the maximal value $|\Delta|_{max}$ of the order parameter in a single-vortex cell [1], and $|\Delta|$ is enhanced near the vortex core [see the inset to Fig. 3(c)]. Both these factors lead to a growth of $\mathbf{j}_s$ near the vortex core [see Eq. (3)]. Therefore, the magnetic moment $\mathbf{m} = (1/2)\int[\mathbf{r} \times \mathbf{j}_s]dS_{cell}$ of each cell in the vortex lattice increases in the LO state.

We base our model on addressing **m** to find M along the direction of B_{ext}, which is an alternative (but much simpler with regard to the role of δg) to using the Gibbs free energy density for the same purpose. Qualitatively, **m** of a given cell creates a dipole magnetic field which in the surrounding cells opposes B_{ext}; hence, an increase of j_s results in a stronger diamagnetic response. Note that the same argument can be used to explain increase of the equilibrium diamagnetism of the mixed state as T decreases. Quantitatively, we have to determine $g(\epsilon)$ and $|\Delta|$. We follow the LO model and solve numerically the modified GL equation for $|\Delta|$ (see Eq. (A49) in [1]) coupled with the equation for $g(\epsilon)$ (see Eq. (A45) in [1]).

In Fig. 3(c), we plot exemplary j_s/j_{GL} vs reduced radial coordinate r/ξ, where $j_{GL} \simeq 0.93\Delta_0(1 - T/T_c)^{1/2}/\xi\rho_n e$ is the equilibrium GL depairing current density, $\Delta_0 \simeq 3.06k_B T_c(1 - T/T_c)^{1/2}$, and ξ corresponds to that at zero vortex velocity u. Results are shown for three different u relative to the LO vortex velocity u_{LO} [1]; the corresponding $|\Delta|/\Delta_0$ is shown in the inset by the same colors. By summing up the resulting **m** of each cell, one can find the difference $\delta M = M_{neq} - M_{eq}$ of the nonequilibrium (M_{neq}) and equilibrium (M_{eq}) magnetization. This is presented in Fig. 3(d). The maximum of $\delta M/M_{eq}$ occurs for $b \sim 0.2$ (at $u/u_{LO} \approx 1$). At smaller b, the enhancement of j_s near the core gives a small contribution to **m**. At larger b, the suppression of $|\Delta|$ at the cell boundary [due to $\delta g(\epsilon) < 0$ for $\epsilon > |\Delta|_{max}$] becomes important. We show results up to $u = 2u_{LO}$, where the LO approach becomes invalid at $T \sim 0.85T_c$.

The spatial variation of M across the boundary between the local lead and the channel occurs over a length of about the intervortex distance $a_0 \approx \sqrt{\phi_0/B_{ext}}$, and induces a current density $\mathbf{j}_M = \nabla \times \mathbf{M}$ that flows along that boundary. This current creates a force $f_M = j_M\phi_0$ that is again *independent* of the direction of I, pulls the vortices toward the local lead (which results in $V_{nl} > 0$), and dominates the total f_{dr} in the SNEQ regime near T_c. The typical $|\delta M| \simeq |M_{eq}| \simeq (B_{c2} - B_{ext})/2.32\mu_0\kappa^2 \simeq 35$ A/m ($\hat{=}45$ μT at $B_{ext} = 0.45$ T) is rather small but appears over a very small distance $a_0(B_{ext} = 0.45$ T$) \simeq 70$ nm, thus providing $j_M \simeq 500$ MA/m² which is of the same order as the transport current densities we used—as $I = 1$ μA corresponds to $j = 100$ MA/m². We again employ Eq. (1) to estimate V_{nl}. Since $j_M = \partial M/\partial x \approx |\delta M|/a_0$ and $X \approx a_0$, with $f_{dr} = f_M$ we obtain

$$V_{nl} = [WB_{ext}a_0/\eta L]j_M\phi_0 = R_{nl}|\delta M|d, \qquad (4)$$

from which a_0 has dropped out again. Inserting typical values of $R_{nl} \approx 0.1$ Ω and $|\delta M| \approx 35$ A/m, we find $V_{nl} \approx 140$ nV, which is quite close to the measured values.

In view of the simplicity of our model, the agreement between the experiment and theory is rather remarkable. A full quantitative account of the phenomenon would require inclusion of other effects on the interface of the local region and the channel—such as details of entry/exit trajectories for the fast and slow vortices, etc. However, these corrections will depend on the individual pinning landscape of the samples. We believe that the main physics of the TFT effect close to T_c is captured by our model.

In conclusion, nonlocal measurements allowed us to qualitatively distinguish two different types of vortex motion in strong nonequilibrium. According to our theory, close to T_c a new type of nonequilibrium magnetization is built up in the region of local drive, which pulls vortices *towards* the local lead. At low temperatures, electron heating leads to a Nernst effect, which pushes vortices *away* from the local lead. Remarkably, this happens irrespective of the sign of the drive current in both cases. The qualitative features as well as the absolute values of the observed nonlocal voltages agree well with the results of our model calculations. Our findings offer a new possibility to probe the presence of vortices or vortexlike excitations as currently discussed in the context of cuprate superconductors [16].

*Present address: attocube systems AG, Germany.
[1] A. I. Larkin and Yu. N. Ovchinnikov, in *Nonequilibrium Superconductivity*, edited by D. N. Langenberg and A. I. Larkin (North Holland, Amsterdam, 1986).
[2] M. N. Kunchur, Phys. Rev. Lett. **89**, 137005 (2002).
[3] M. N. Kunchur, B. I. Ivlev, and J. M. Knight, Phys. Rev. Lett. **87**, 177001 (2001).
[4] D. Babić, in *New Frontiers in Superconductivity Research*, edited by B. S. Martins (Nova Science Publishers, New York, 2006).
[5] D. Babić *et al.*, Phys. Rev. B **69**, 092510 (2004).
[6] I. V. Grigorieva *et al.*, Phys. Rev. Lett. **92**, 237001 (2004).
[7] A. Helzel *et al.*, Phys. Rev. B **74**, 220510(R) (2006).
[8] F. Otto, Ph.D. thesis Universitätsverlag Regensburg, 2008; see EPAPS supplementary material at http://link.aps.org/supplemental/10.1103/PhysRevLett.104.027005 for analysis of local $V(I)$; for the noise measurement method, see M. Henny *et al.*, Phys. Rev. B **59**, 2871 (1999).
[9] Pinning reduces R_{nl} through a modified η.
[10] R. P. Huebener, *Magnetic Flux Structures in Superconductors* (Springer, New York, 2001).
[11] K. Maki, J. Low Temp. Phys. **1**, 45 (1969).
[12] N. B. Kopnin, J. Low Temp. Phys. **93**, 117 (1993).
[13] R. P. Huebener and A. Seher, Phys. Rev. **181**, 701 (1969).
[14] F. Vidal, Phys. Rev. B **8**, 1982 (1973).
[15] A. Schmid, G. Schön, and M. Tinkham, Phys. Rev. B **21**, 5076 (1980).
[16] See, e.g., I. Kokanović, J. R. Cooper, and M. Matusiak, Phys. Rev. Lett. **102**, 187002 (2009).